Foam Rheology Near the Jamming Transition

Woldhuis, E.L.

Chapter 7

Non-linear Scaling Model

All of the preceding chapters dealt with a linear microscopic model: the elastic forces of Eq. 2.1 and the viscous forces of Eq. 2.3 are linear in respectively the overlap and the relative velocity. There are two good reasons to consider a larger class of microscopic models. The first reason is that many systems, for example the foams that we claim to describe, do not actually have linear (viscous) interactions. The second reason is that this allows us to probe whether changing the microscopic interactions influences the critical exponents. Given the way we have derived our 'critical' exponents, it does not seem likely that our exponents are independent of the microscopic interactions, and this aspect will be investigated in detail in this chapter.

7.1 Microscopic Model

We generalise our original, linear, microscopic model by changing the interactions into more general power law dependences:

$$\mathbf{F}^{\mathrm{e}}_{ij} = k\delta_{ij}^{\alpha_{\mathrm{e}}}\hat{\mathbf{r}} \tag{7.1}$$

$$\mathbf{F}^{\mathrm{v}}_{ij} = -b\Delta v_{ij}^{\alpha_{\mathrm{v}}}\Delta\hat{\mathbf{v}}_{ij}, \tag{7.2}$$

with $\hat{\mathbf{r}}$ the unit vector connecting the centres of particles i and j and α_{e} and α_{v} being general power law exponents that can take any (positive) value. Note that both forces will still be zero when particles are not in contact and that setting $\alpha_{\mathrm{e}} = \alpha_{\mathrm{v}} = 1$ recovers the linear Durian model of the preceding chapters. This new formulation will allow our model to describe many more experimentally relevant systems. For example, the model can describe hertzian particles like grains in which $F^{\mathrm{e}} \sim \delta^{3/2}$. More importantly, foams do not have linear viscous interactions, but are microscopically shear thinning, $F \sim \Delta v^{2/3}$ [37]. Our new model can therefore make predictions for the rheology of these kinds of systems. These predictions will be developed and tested in this chapter.

7.2 Scaling Model

We will now investigate how the three ingredients of our original 3E scaling model, power balance Eq. 4.1, effective strain Eq. 4.2 and the elasticity relation Eq. 4.5, change when we change from the linear microscopic model to the more general power law microscopic model.

7.2.1 Energy Balance

The first ingredient of our 3E model is an equation for power balance. The power that is put into a system of linear size L by shearing is given by $\sigma_{xy}\dot{\gamma}L^2$. This power is dissipated by the viscous interactions between the bubbles. The power that is dissipated between two bubbles, i and j, is given by $\Delta\mathbf{v}_{ij}\cdot\mathbf{F}^{\mathrm{v}}_{ij}$, the inner product of their relative velocity and the dissipative force they exert on each other. Averaging both expressions over time and averaging the dissipation over all contacts then yields

$$\langle\sigma_{xy}\rangle_t \dot{\gamma}L^2 = N/2 \left\langle Z \left\langle \Delta\mathbf{v}_{ij}\cdot\mathbf{F}^{\mathrm{v}}_{ij}\right\rangle_{ij}\right\rangle_t, \tag{7.3}$$

with $\langle\cdot\rangle_{ij}$ indicating averaging over all contacts. Since the viscous force is so explicitly present in the formulation of power balance, it is clear that, and how, changing the exponent of the viscous force will change the formulation of power balance. Substituting our definition for the dissipative force, equation 7.2, we get the following expression:

$$\langle\sigma_{xy}\rangle_t \dot{\gamma}L^2 = bN/2 \left\langle Z \left\langle \Delta\mathbf{v}^{1+\alpha_{\mathrm{v}}}\right\rangle_{ij}\right\rangle_t, \tag{7.4}$$

7.2.2 Effective Strain

The effective strain will not depend explicitly on the microscopic force laws in our system: the yield strain, γ_{y}, is a function of the compression only and while the way the compression depends on, for example, the pressure may depend on the microscopic interactions, the formulation of the effective strain as a function of $\Delta\phi$ will not. Similarly, the dynamic strain, γ_{dyn}, depends on the timescale in which particles rearrange, which itself depends on the strain rate with which the system is driven and the average relative velocity between particles. Although the average relative velocity will probably not be the same in systems with different microscopic force laws, the way the dynamic strain depends on this difference is purely geometric and therefore will not change.

This means that we can simply copy the relation that we had before:

$$\gamma_{\mathrm{y}} = \Delta\phi \tag{7.5}$$

$$\gamma_{\mathrm{dyn}} = \frac{\dot{\gamma} d}{\langle \Delta v \rangle_{t,ij}} \tag{7.6}$$

$$\gamma_{\mathrm{eff}}^{xy} = B_{\mathrm{eff}}^{xy} \gamma_{\mathrm{y}} + \gamma_{\mathrm{dyn}} \tag{7.7}$$

$$\gamma_{\mathrm{eff}}^{xx} = B_{\mathrm{eff}}^{xx} \gamma_{\mathrm{y}} + \gamma_{\mathrm{dyn}} \tag{7.8}$$

7.2.3 Elasticity Relation

The situation for the elasticity is more complicated. It will turn out to depend on the elastic force law, but not in such a straightforward way as our power balance expression depended on the viscous force law. In order to derive this dependence we start by looking at the dimensionless stress. In the linear case we had the following expression

$$\tilde{\sigma} = \frac{\sigma}{k} \tag{7.9}$$

In our non-linear microscopic model, however, the unit of k is no longer Nm^{-1} but $Nm^{-\alpha_{\mathrm{e}}}$ and the resulting $\tilde{\sigma}$ is not dimensionless. Therefore, we need to formulate a more general expression for the dimensionless stress which reduces to Eq. 7.9 for linear interactions but gives a dimensionless stress for all values of α_{e} (and α_{v}). One possible approach is to divide not by the bare spring constant k, but by the effective spring constant $k_{\mathrm{eff}} = \langle \mathrm{d}F^{\mathrm{e}}/\mathrm{d}\delta \rangle_{ij} = \left\langle \alpha_{\mathrm{e}} k \delta^{\alpha_{\mathrm{e}}-1} \right\rangle$, which will always have units of Nm^{-1}. Note that in the linear case $k_{\mathrm{eff}} = k$. If we assume that the typical overlap will scale with the global effective strain and the particle size, we get:

$$k_{\mathrm{eff}} = \alpha_{\mathrm{e}} k \left(d\gamma_{\mathrm{eff}} \right)^{\alpha_{\mathrm{e}}-1} \tag{7.10}$$

We also assume that the non-dimensional stress will still depend on the effective strain in the same way as in the linear case, Eqs. 4.5 and 5.4. Especially in the case of the normal stress, where our elasticity equation was purely phenomenological, this is a strong assumption. We must first give the elasticity relation in non-dimensional form, but since we only have to divide by k in the linear case, this is straightforward:

$$\tilde{\sigma}_{xy}^{\mathrm{e}} = A_1^{xy} \Delta\phi^{1/2} \gamma_{\mathrm{eff}}^{xy} \sqrt{1 + \frac{\left(A_2^{xy} \gamma_{\mathrm{eff}}^{xy} \right)^2}{\Delta\phi}} \tag{7.11}$$

$$\tilde{\sigma}_{xx}^{\mathrm{e}} = A_1^{xx} \gamma_{\mathrm{eff}}^{xx\,1.3}. \tag{7.12}$$

Multiplying this with k_{eff} to recover the expression for the full, dimensional

	Critical			Transition		
elasticity	σ	$\sim$	$\gamma_{\text{eff}}^{1+\alpha_e}$	σ	$\sim$	$\Delta\phi^{1/2}\gamma_{\text{eff}}^{\alpha_e}$
effective strain	γ_{eff}	$\sim$	$\dot{\gamma}/\Delta v$	γ_{eff}	$\sim$	$\dot{\gamma}/\Delta v$
rheology	σ	$\sim$	$\dot{\gamma}^{\frac{\alpha_v(1+\alpha_e)}{2+\alpha_v+\alpha_e}}$	σ	$\sim$	$\Delta\phi^{\frac{1+\alpha_v}{2(1+\alpha_v+\alpha_e)}}\dot{\gamma}^{\frac{\alpha_e\alpha_v}{1+\alpha_v+\alpha_e}}$
range	$\dot{\gamma}$	$>$	$\Delta\phi^{\frac{2+\alpha_v+\alpha_e}{2\alpha_v}}$	$\dot{\gamma}$	$>$	$\Delta\phi^{\frac{3/2+\alpha_v+\alpha_e}{\alpha_v}}$
	$\dot{\gamma}$	$>$	$\Delta\phi^{2+\alpha_v+\alpha_e}$	$\dot{\gamma}$	$<$	$\Delta\phi^{\frac{2+\alpha_v+\alpha_e}{2\alpha_v}}$
	Yield			Dense		
elasticity	σ	$\sim$	$\Delta\phi^{1/2}\gamma_{\text{eff}}^{\alpha_e}$	σ	$\sim$	$\gamma_{\text{eff}}^{1+\alpha_e}$
effective strain	γ_{eff}	$\sim$	$\Delta\phi$	γ_{eff}	$\sim$	$\Delta\phi$
rheology	σ	$\sim$	$\Delta\phi^{\alpha_e+1/2}$	σ	$\sim$	$\Delta\phi^{\alpha_e+1}$
range	$\dot{\gamma}$	$<$	$\Delta\phi^{\frac{3/2+\alpha_v+\alpha_e}{\alpha_v}}$	C	$<$	$\Delta\phi$
	C	$>$	$\Delta\phi$	$\dot{\gamma}$	$<$	$\Delta\phi^{2+\alpha_v+\alpha_e}$

Table 7.1: The four rheological regimes for the shear stress in our general power law scaling model with their definitions, results and ranges of validity.

stress we get:

$$\sigma_{xy}^{\text{e}} = A_1^{xy}\alpha_e k d^{\alpha_e-1}\Delta\phi^{1/2}\gamma_{\text{eff}}^{xy\alpha_e}\sqrt{1+\frac{\left(A_2^{xy}\gamma_{\text{eff}}^{xy}\right)^2}{\Delta\phi}} \tag{7.13}$$

$$\sigma_{xx}^{\text{e}} = A_1^{xx}\alpha_e k d^{\alpha_e-1}\gamma_{\text{eff}}^{xx\alpha_e+0.3}. \tag{7.14}$$

7.3 Regimes

Now that we have our three scaling model ingredients for the general power law case, we note two things. First, both microscopic force law exponents enter in them and will therefore presumably impact the rheology. Second, there are still two regimes for the effective strain, Eq. 7.5 and two, respectively one, regimes for the shear, respectively normal, stress elasticity, Eq. 7.13, 7.14. This means that we can still apply the same methodology as in the linear case: we divide the full parameter space in four, for the shear stress, and three, for the normal stress, regimes, as indicated in table 7.1; then solve the rheological relations by simple substitution in each regime and finally use these results to determine the crossovers between the regimes. While the resulting exponents will be more involved, featuring fractions and combinations of α_e and α_v, the methods are completely similar to those used in section 3.2. Therefore, the rheological results are presented in tables 7.1 and 7.2. In the section below we list the full results, including expressions for Δv and γ_{eff}.

	Normal Critical			Normal Transition		
shear stress	σ_{xy}	$\sim$	$\dot{\gamma}^{\frac{\alpha_v(1+\alpha_e)}{2+\alpha_v+\alpha_e}}$	σ_{xy}	$\sim$	$\Delta\phi^{\frac{1+\alpha_v}{2(1+\alpha_v+\alpha_e)}}\dot{\gamma}^{\frac{\alpha_e\alpha_v}{1+\alpha_v+\alpha_e}}$
effective strain	γ_{eff}	$\sim$	$\dot{\gamma}/\Delta v$	γ_{eff}	$\sim$	$\dot{\gamma}/\Delta v$
rheology	σ_{xx}	$\sim$	$\dot{\gamma}^{\frac{\alpha_v(\alpha_e+0.3)}{2+\alpha_v+\alpha_e}}$	σ_{xx}	$\sim$	$\Delta\phi^{\frac{-(\alpha_e+0.3)}{2(1+\alpha_v+\alpha_e)}}\dot{\gamma}^{\frac{\alpha_v(\alpha_e+0.3)}{1+\alpha_v+\alpha_e}}$
range	$\dot{\gamma}$	$>$	$\Delta\phi^{\frac{2+\alpha_v+\alpha_e}{2\alpha_v}}$	$\dot{\gamma}$	$>$	$\Delta\phi^{\frac{3/2+\alpha_v+\alpha_e}{\alpha_v}}$
				$\dot{\gamma}$	$<$	$\Delta\phi^{\frac{2+\alpha_v+\alpha_e}{2\alpha_v}}$

	Normal Yield		
effective strain	γ_{eff}	$\sim$	$\Delta\phi$
rheology	σ_{xx}	$\sim$	$\Delta\phi^{\alpha_e+0.3}$
range	$\dot{\gamma}$	$<$	$\Delta\phi^{\frac{3/2+\alpha_v+\alpha_e}{\alpha_v}}$

Table 7.2: The three rheological regimes for the normal stress with their definitions, results and ranges of validity. Note that the shear stress enters as one of the ingredients that determines the regime.

7.3.1 Shear Stress

Yield Regime We will start with the shear stress in the Yield regime. The definition of this regime is the same as in the linear case: the effective strain, Eq. 7.5, is dominated by the yield contribution and the elasticity relation, Eq. 7.13, is dominated by the linear contribution:

$$\begin{cases} \sigma\dot{\gamma} \sim \Delta v^{1+\alpha_v} \\ \gamma_{\text{eff}} \sim \Delta\phi \\ \sigma_{xy} \sim \Delta\phi^{1/2}\gamma_{\text{eff}}^{\alpha_e} \end{cases} \Rightarrow \begin{cases} \Delta v \sim \dot{\gamma}^{\frac{1}{1+\alpha_v}}\Delta\phi^{\frac{2\alpha_e+1}{2(1+\alpha_v)}} \\ \gamma_{\text{eff}} \sim \Delta\phi \\ \sigma_{xy} \sim \Delta\phi^{\alpha_e+1/2} \end{cases} \tag{7.15}$$

Not surprisingly, the stress in the Yield regime, in which the material is thought to exhibit elastic behavior, depends on the elastic but not the viscous exponent. Also note that all relations reduce to their linear equivalents, found in Eq. 3.14, if we take $\alpha_e = \alpha_v = 1$.

Transition Regime In the Transition regime, the elasticity relation is dominated by the linear contribution, but the effective strain is dominated by the dynamic contribution:

$$\begin{cases} \sigma\dot{\gamma} \sim \Delta v^{1+\alpha_v} \\ \gamma_{\text{eff}} \sim \dot{\gamma}/\Delta v \\ \sigma_{xy} \sim \Delta\phi^{1/2}\gamma_{\text{eff}}^{\alpha_e} \end{cases} \Rightarrow \begin{cases} \Delta v \sim \Delta\phi^{\frac{1}{2(1+\alpha_v+\alpha_e)}}\dot{\gamma}^{\frac{1+\alpha_e}{1+\alpha_v+\alpha_e}} \\ \gamma_{\text{eff}} \sim \Delta\phi^{\frac{-1}{2(1+\alpha_v+\alpha_e)}}\dot{\gamma}^{\frac{v}{1+\alpha_v+\alpha_e}} \\ \sigma_{xy} \sim \Delta\phi^{\frac{1+\alpha_v}{2(1+\alpha_v+\alpha_e)}}\dot{\gamma}^{\frac{\alpha_v\alpha_e}{1+\alpha_v+\alpha_e}} \end{cases} \tag{7.16}$$

Due to the, appearance of both α_v and α_e these expressions look rather unappealing. Still, it is again easy to check that substituting $\alpha_\mathrm{v} = \alpha_\mathrm{e} = 1$ recovers the linear expressions of Eq. 3.15.

Critical Regime In the Critical regime, the elasticity is dominated by the non-linear contribution and the effective strain is dominated by the dynamic strain:

$$\begin{cases} \sigma\dot{\gamma} \sim \Delta v^{1+\alpha_\mathrm{v}} \\ \gamma_\mathrm{eff} \sim \frac{\dot{\gamma}}{\Delta v} \\ \sigma_{xy} \sim \gamma_\mathrm{eff}^{1+\alpha_\mathrm{e}} \end{cases} \Rightarrow \begin{cases} \Delta v \sim \dot{\gamma}^{\frac{2+\alpha_\mathrm{e}}{2+\alpha_\mathrm{v}+\alpha_\mathrm{e}}} \\ \gamma_\mathrm{eff} \sim \dot{\gamma}^{\frac{\alpha_\mathrm{v}}{2+\alpha_\mathrm{v}+\alpha_\mathrm{e}}} \\ \sigma_{xy} \sim \dot{\gamma}^{\frac{\alpha_\mathrm{v}(1+\alpha_\mathrm{e})}{2+\alpha_\mathrm{v}+\alpha_\mathrm{e}}} \end{cases} \tag{7.17}$$

Again, the expressions are unappealing but reduce to the linear results of Eq. 3.13 for $\alpha_\mathrm{v} = \alpha_\mathrm{e} = 1$.

Dense Regime For completeness' sake we also give the results for the inaccessible Dense regime:

$$\begin{cases} \sigma\dot{\gamma} \sim \Delta v^{1+\alpha_\mathrm{v}} \\ \gamma_\mathrm{eff} \sim \Delta\phi \\ \sigma_{xy} \sim \gamma_\mathrm{eff}^{1+\alpha_\mathrm{e}} \end{cases} \Rightarrow \begin{cases} \Delta v \sim \Delta\phi^{\frac{1+\alpha_\mathrm{e}}{1+\alpha_\mathrm{v}}} \dot{\gamma}^{\frac{1}{1+\alpha_\mathrm{v}}} \\ \gamma_\mathrm{eff} \sim \Delta\phi \\ \sigma_{xy} \sim \Delta\phi^{\alpha_\mathrm{e}+1} \end{cases} \tag{7.18}$$

Crossovers

Now that we have the rheological behavior in all four regimes, we can derive expression for the crossovers between the various regimes. These will again depend on the exponents α_e and α_v. The methodology is the same as in the linear case, equating the expressions for the stress in two regimes, though the exponents will be more involved; they are given in table 7.1

We start by comparing the stress in the Yield and the Transition regime:

$$\Delta\phi^{\alpha_\mathrm{e}+1/2} \sim \Delta\phi^{\frac{1+\alpha_\mathrm{v}}{2(1+\alpha_\mathrm{v}+\alpha_\mathrm{e})}} \dot{\gamma}^{\frac{\alpha_\mathrm{v}\alpha_\mathrm{e}}{1+\alpha_\mathrm{v}+\alpha_\mathrm{e}}} \Rightarrow \dot{\gamma} \sim \Delta\phi^{\frac{3/2+\alpha_\mathrm{v}+\alpha_\mathrm{e}}{\alpha_\mathrm{v}}} . \tag{7.19}$$

The next crossover, from the Transition to the Critical regime, we find by comparing the expressions for the stress in those two regimes:

$$\Delta\phi^{\frac{1+\alpha_\mathrm{v}}{2(1+\alpha_\mathrm{v}+\alpha_\mathrm{e})}} \dot{\gamma}^{\frac{\alpha_\mathrm{v}\alpha_\mathrm{e}}{1+\alpha_\mathrm{v}+\alpha_\mathrm{e}}} \sim \dot{\gamma}^{\frac{\alpha_\mathrm{v}(1+\alpha_\mathrm{e})}{2+\alpha_\mathrm{v}+\alpha_\mathrm{e}}} \Rightarrow \dot{\gamma} \sim \Delta\phi^{\frac{2+\alpha_\mathrm{v}+\alpha_\mathrm{e}}{2\alpha_\mathrm{v}}} . \tag{7.20}$$

Note that the exponent of the density here, $(2 + \alpha_\mathrm{v} + \alpha_\mathrm{e})/2\alpha_\mathrm{v}$, is always smaller than the exponent of the density in the Yield-to-Transition crossover, $(3/2 + \alpha_\mathrm{v} + \alpha_\mathrm{e})/\alpha_\mathrm{v}$, independent of α_v and α_e. Therefore: for every (positive) value of α_e and α_v, when the density is small, we will first crossover from the Yield to the Transition regime and then from the Transition to the Critical

regime when $\dot{\gamma}$ is increased. Of course, we had already seen that this was so for the specific case of $\alpha_\mathrm{e} = \alpha_\mathrm{v} = 1$; now we know that this behavior is general.

The crossover from the Yield to the Dense regime still takes place at a fixed density:

$$\Delta\phi^{\alpha_\mathrm{e}+1/2} \sim \Delta\phi^{\alpha_\mathrm{e}+1} \Rightarrow \Delta\phi \sim 1 \ , \tag{7.21}$$

this 'derivation' makes it clear that changing α_v or α_e will not impact this result.

For the final crossover, form the Dense to the Critical regime, we find:

$$\Delta\phi^{\alpha_\mathrm{e}+1} \sim \dot{\gamma}^{\frac{\alpha_\mathrm{v}(1+\alpha_\mathrm{e})}{2+\alpha_\mathrm{v}+\alpha_\mathrm{e}}} \Rightarrow \dot{\gamma} \sim \Delta\phi^{\frac{2+\alpha_\mathrm{v}+\alpha_\mathrm{e}}{\alpha_\mathrm{v}}} \ . \tag{7.22}$$

As already mentioned above, changing the exponents will also change the crossovers *quantitatively*, but will not change the nature of the crossovers *qualitatively*. The general trends shown in figure 3.1 are therefore applicable to all exponents.

7.3.2 Normal Stress

As in the linear case, the rheology for the normal stress is somewhat special because the expressions for the shear stress that we derived above enter through energy balance. This causes the appearance of a third regime, even though there is only one ingredient with two regimes. We summarise the results for the stress in table 7.2 and present the full results below. Note that, just like the linear case $\langle \Delta v \rangle$ is set by the shear behavior and not by the normal behavior.

Normal Yield For the Normal Yield regime we have:

$$\begin{cases} \sigma_{xy}\dot{\gamma} \sim \Delta v^{1+\alpha_\mathrm{v}} \\ \gamma_\mathrm{eff} \sim \Delta\phi \\ \sigma_{xx} \sim \gamma_\mathrm{eff}^{\alpha_\mathrm{e}+0.3} \\ \sigma_{xy} \sim \gamma_\mathrm{eff}^{\alpha_\mathrm{e}+1/2} \end{cases} \Rightarrow \begin{cases} \Delta v \sim \dot{\gamma}^{\frac{1}{1+\alpha_\mathrm{v}}} \Delta\phi^{\frac{2\alpha_\mathrm{e}+1}{2(1+\alpha_\mathrm{v})}} \\ \gamma_\mathrm{eff} \sim \Delta\phi \\ \sigma_{xx} \sim \Delta\phi^{\alpha_\mathrm{e}+0.3} \end{cases} \tag{7.23}$$

Normal Transition In the Normal Transition regime we have:

$$\begin{cases} \sigma_{xy}\dot{\gamma} \sim \Delta v^{1+\alpha_\mathrm{v}} \\ \gamma_\mathrm{eff} \sim \frac{\dot{\gamma}}{\langle \Delta v \rangle} \\ \sigma_{xx} \sim \gamma_\mathrm{eff}^{\alpha_\mathrm{e}+0.3} \\ \sigma_{xy} \sim \Delta\phi^{\frac{1+\alpha_\mathrm{v}}{2(1+\alpha_\mathrm{v}+\alpha_\mathrm{e})}} \dot{\gamma}^{\frac{\alpha_\mathrm{v}\alpha_\mathrm{e}}{1+\alpha_\mathrm{v}+\alpha_\mathrm{e}}} \end{cases} \Rightarrow \begin{cases} \Delta v \sim \Delta\phi^{\frac{1}{2(1+\alpha_\mathrm{v}+\alpha_\mathrm{e})}} \dot{\gamma}^{\frac{1+\alpha_\mathrm{e}}{1+\alpha_\mathrm{v}+\alpha_\mathrm{e}}} \\ \gamma_\mathrm{eff} \sim \Delta\phi^{\frac{-1}{2(1+\alpha_\mathrm{v}+\alpha_\mathrm{e})}} \dot{\gamma}^{\frac{\alpha_\mathrm{v}}{1+\alpha_\mathrm{v}+\alpha_\mathrm{e}}} \\ \sigma_{xx} \sim \Delta\phi^{\frac{-(\alpha_\mathrm{e}+0.3)}{2(1+\alpha_\mathrm{v}+\alpha_\mathrm{e})}} \dot{\gamma}^{\frac{\alpha_\mathrm{v}(\alpha_\mathrm{e}+0.3)}{1+\alpha_\mathrm{v}+\alpha_\mathrm{e}}} \end{cases} \tag{7.24}$$

Regime Combination			rescaled axes		
Critical	and	Transition	$\sigma/\Delta\phi^{\frac{1+\alpha_e}{2}}$	vs.	$\dot\gamma/\Delta\phi^{\frac{2+\alpha_v+\alpha_e}{2\alpha_v}}$
Yield	and	Transition	$\sigma/\Delta\phi^{\alpha_e+1/2}$	vs.	$\dot\gamma/\Delta\phi^{\frac{3/2+\alpha_e+\alpha_v}{\alpha_v}}$
Yield	and	Critical	$\sigma/\Delta\phi^{\alpha_e+1/2}$	vs.	$\dot\gamma/\Delta\phi^{\frac{(\alpha_e+1/2)(2+\alpha_v+\alpha_e)}{\alpha_v(1+\alpha_e)}}$

Table 7.3: Prescriptions of what to plot for collapse in the indicated regimes.

Regime Combination			rescaled axes		
Normal Critical	and	Normal Transition	$\sigma/\Delta\phi^{\frac{\alpha_e+0.3}{2}}$	vs.	$\dot\gamma/\Delta\phi^{\frac{2+\alpha_v+\alpha_e}{2\alpha_v}}$
Normal Yield	and	Normal Transition	$\sigma/\Delta\phi^{\alpha_e+0.3}$	vs.	$\dot\gamma/\Delta\phi^{\frac{3/2+\alpha_e+\alpha_v}{\alpha_v}}$
Normal Yield	and	Normal Critical	$\sigma/\Delta\phi^{\alpha_e+0.3}$	vs.	$\dot\gamma/\Delta\phi^{\frac{2+\alpha_v+\alpha_e}{\alpha_v}}$

Table 7.4: Prescriptions of what to plot for collapse of the normal stress in the indicated regimes.

Normal Critical In the Normal critical regime we have:

$$\begin{cases} \sigma_{xy}\dot\gamma \sim \Delta v^{1+\alpha_v} \\ \gamma_{\text{eff}} \sim \frac{\dot\gamma}{\langle\Delta v\rangle} \\ \sigma_{xx} \sim \gamma_{\text{eff}}^{\alpha_e+0.3} \\ \sigma_{xy} \sim \dot\gamma^{\frac{\alpha_v(1+\alpha_e)}{2+\alpha_v+\alpha_e}} \end{cases} \Rightarrow \begin{cases} \Delta v \sim \dot\gamma^{\frac{2+\alpha_e}{2+\alpha_v+\alpha_e}} \\ \gamma_{\text{eff}} \sim \dot\gamma^{\frac{\alpha_v}{2+\alpha_v+\alpha_e}} \\ \sigma_{xx} \sim \dot\gamma^{\frac{\alpha_v(\alpha_e+0.3)}{2+\alpha_v+\alpha_e}} \end{cases} \tag{7.25}$$

Crossovers

The crossovers for the normal stress are simply inherited from the crossovers of the shear stress, just like in the linear case.

7.4 Plotting

Since the general structure of the rheology has not changed: three (accessible) regimes, power laws of strain rate and density, we can still hope to plot the rheological curves as we could in the linear case: collapsed by rescaling with the density. Short derivations will be presented in the section below, but the important results are summarized in tables 7.3 and 7.4

7.4.1 Shear Stress

For the shear stress there are, realistically, three regimes. This means that, as before, it will not be possible to collapse the full curve, at best we can rescale

two regimes. Below we will discuss the rescaling with $\Delta\phi$ that is necessary to get collapse in each combination of two regimes.

Yield and Transition If we want to attain collapse in the Yield and Transition regimes we start by looking at the stress in the Yield regime: it depends on density, but not on the strain rate. Therefore the only way to get the stress to collapse in the Yield regime is by picking the correct rescaling in the stress. Since the stress in the Yield regime is given by $\sigma_{xy} \sim \Delta\phi^{\alpha_e+1/2}$, we have $\tilde{\sigma}_{xy} \sim \sigma_{xy}/\Delta\phi^{\alpha_e+1/2}$. In addition, we rescale the $\dot{\gamma}$-axis with the $\Delta\phi$ dependence of the crossover so that we get collapse there as well: $\tilde{\dot{\gamma}} \sim \dot{\gamma}/\Delta\phi^{(3/2+\alpha_e+\alpha_v)/\alpha_v}$. As in the linear case this will automatically result in collapse in the Transition regime as well.

Transition and Critical To get collapse in both the Critical and the Transition regime, the first thing we must do is collapse the crossover by plotting $\tilde{\dot{\gamma}} \sim \dot{\gamma}/\Delta\phi^{(2+\alpha_v+\alpha_e)/2\alpha_v}$. With this relation we can now derive how we need to plot the stress to get collapse in the Critical regime:

$$\sigma_{xy} \sim \dot{\gamma}^{\frac{\alpha_v(1+\alpha_e)}{2+\alpha_v+\alpha_e}} = \tilde{\dot{\gamma}}^{\frac{\alpha_v(1+\alpha_e)}{2+\alpha_v+\alpha_e}} \Delta\phi^{\frac{\alpha_v(1+\alpha_e)}{2\alpha_v}} \Rightarrow \tilde{\sigma}_{xy} \sim \sigma_{xy}/\Delta\phi^{\frac{\alpha_v(1+\alpha_e)}{2\alpha_v}} \tag{7.26}$$

Again, this will also give collapse in the Transition regime.

Yield and Critical Again we need to plot $\tilde{\sigma}_{xy} \sim \sigma_{xy}/\Delta\phi^{\alpha_e+1/2}$ for collapse of the Yield stress. We substitute this expression into the rheological relation for the Critical regime to find the required strain rate rescaling:

$$\sigma_{xy} \sim \dot{\gamma}^{\frac{\alpha_v(1+\alpha_e)}{2+\alpha_v+\alpha_e}} \Rightarrow \tilde{\sigma}_{xy} \sim \dot{\gamma}^{\frac{\alpha_v(1+\alpha_e)}{2+\alpha_v+\alpha_e}}/\Delta\phi^{\alpha_e+1/2} \Rightarrow \tilde{\dot{\gamma}} \sim \dot{\gamma}/\Delta\phi^{\frac{(\alpha_e+1/2)(2+\alpha_v+\alpha_e)}{\alpha_v(1+\alpha_e)}}. \tag{7.27}$$

This will not result in collapse in either the Transition regime, of the crossover from the Yield to the Transition regime or of the crossover from the Transition to the Critical regime.

7.4.2 Normal Stress

Plotting the normal stress will be similar to the shear stress in some cases, because the same crossovers need to be collapsed, but different in most cases, since the stress scales differently.

Normal Yield and Normal Transition Regimes As mentioned above, the strain rate needs to be rescaled to make the crossover between the Normal Yield and Normal Transition regimes, which is the same as for the shear tress, collapse: $\tilde{\dot{\gamma}} \sim \dot{\gamma}/\Delta\phi^{(3/2+\alpha_e+\alpha_v)/\alpha_v}$. Since the stress in the Normal Yield regime depends only on the density, this prescribes the rescaling of the stress: $\sigma_{xx} \sim \Delta\phi^{\alpha_e+0.3}$.

Normal Transition and Normal Critical Regimes Between the Normal Transition and the Normal Critical regime there is a crossover that determines the strain rate rescaling: $\tilde{\dot{\gamma}} \sim \dot{\gamma}/\Delta\phi^{(2+\alpha_v+\alpha_e)/2\alpha_v}$. Substituting this into the expression for the stress in the Normal Critical regime yields:

$$\sigma_{xx} \sim \dot{\gamma}^{\frac{\alpha_v(\alpha_e+0.3)}{2+\alpha_v+\alpha_e}} = \tilde{\dot{\gamma}}^{\frac{\alpha_v(\alpha_e+0.3)}{2+\alpha_v+\alpha_e}} \Delta\phi^{\frac{\alpha_e+0.3}{2}} \Rightarrow \tilde{\sigma}_{xx} \sim \sigma_{xx}/\Delta\phi^{\frac{\alpha_e+0.3}{2}}. \quad (7.28)$$

Normal Yield and Normal Critical Regimes Again, the dependence of the Normal Yield stress on the density prescribes the rescaling of the stress: $\sigma_{xx} \sim \Delta\phi^{\alpha_e+0.3}$. This can be substituted into the expression for the stress in the Critical regime to deduce the rescaling of the strain rate:

$$\sigma_{xx} \sim \dot{\gamma}^{\frac{\alpha_v(\alpha_e+0.3)}{2+\alpha_v+\alpha_e}} \Rightarrow \tilde{\sigma}_{xx} \sim \dot{\gamma}^{\frac{\alpha_v(\alpha_e+0.3)}{2+\alpha_v+\alpha_e}}/\Delta\phi^{\alpha_e+0.3} \Rightarrow \tilde{\dot{\gamma}} \sim \dot{\gamma}/\Delta\phi^{\frac{2+\alpha_v+\alpha_e}{\alpha_v}} \quad (7.29)$$

7.5 Experimental Implementations

Now we will compare the predictions from our scaling model with previous experiments done by other people. Since our model describes a much wider array of systems than artificial linear model, we will be able to accurately describe real systems. We will compare our model to experimental data of flowing foams by Katgert *et al.* [37] and experimental data of colloid rheology by Nordstrom *et al.* [39] .These two systems also have the advantage of being theoretically interesting because they decouple the effects of non-linear elasticity and non-linear viscosity. This is because the foam system has linear elasticity but non-linear viscosity, $\alpha_v = 2/3$, while the colloid system has linear viscosity but non-linear elasticity, $\alpha_e = 3/2$.

7.5.1 Katgert Foam Data

We start by looking at systems of flowing foam, the system we had in our mind when developing the original linear model. For this we can use experiments performed by Gijs Katgert *et al.* In the experiments, a two dimensional bubble layer is confined between the liquid surface on the bottom and a glass plate on top. Two large wheels then apply a constant strain rate to the system, bringing it in steady shear. A picture of the setup is given in figure 7.1. In this system, Katgert can modify the strain rate and, within a narrow range, the density.

An important difference between the system of Katgert *et al.* and our system is the presence of a top plate. The top plate exerts a drag force on all bubbles. Since this drag force depends on the velocities of the bubbles with respect to this top plate, there is an additional energetic penalty to high velocities, which results in shear banding. In effect, the top plate breaks galilean symmetry and enforces the laboratory frame as a special frame.

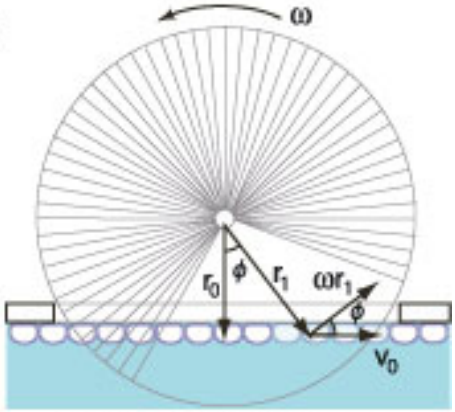

Figure 7.1: Figure from [37]. Side view of the setup used by Katgert *et al.*

In spite of this, Katgert has developed a model that allows him to take, amongst other things, the degree of shear banding and get out the 'pure' rheological behavior: the dependence of the required shear stress on the applied strain rate: he gets a good fit for Herschell-Bulkley behavior:

$$\sigma_{xy} \sim \sigma_Y + \dot{\gamma}^{0.36}, \tag{7.30}$$

where σ_Y is a yield stress. Our model should predict, then, that the exponent with which the shear stress depends on the strain rate in the Critical regime has a value 0.36 ± 0.05, taking into account he error bars on the experimental result. In what follows we will call this exponent β to facilitate the discussion. In order to see if our model indeed predicts $\beta = 0.36$, we need to know the exponents in the force laws between the individual bubbles, $\alpha_{\rm e}$ and $\alpha_{\rm v}$.

According to Katgert, his bubbles have linear elastic interactions, $\alpha_{\rm e} = 1$, but non-linear viscous interactions. He measures their viscous interactions to follow $\alpha_{\rm v} = 2/3$ [37]. If we substitute these two values into the expression we derived for the stress in the Critical regime, Eq. 7.17, we find:

$$\sigma_{xy} \sim \dot{\gamma}^{\frac{\alpha_{\rm v}(1+\alpha_{\rm e})}{2+\alpha_{\rm v}+\alpha_{\rm e}}} = \dot{\gamma}^{\frac{4/3}{3+2/3}} = \dot{\gamma}^{4/11} = \dot{\gamma}^{0.36}, \tag{7.31}$$

which is in excellent agreement with the experimental value of 0.36 ± 0.05.

Of course, there are some caveats. First of all, the fact that the exponents match so closely cannot be attributed to anything besides luck because there are considerable experimental error bars on both $\alpha_{\rm v}$ and β, and Katgert *et al.* present a number of slightly different values in a later paper [34]. Still this does not change the result that our model prediction for β is consistent with the experiment.

Second, and slightly more problematic, is the apparent lack of a Transition regime in the data of Katgert *et al.* ; while our model predicts three regimes,

Katgert only finds two. We claim that this is reasonable because the Transition regime can be hard to pin down experimentally: it can be very small, as we have seen in section 4.4.1, and the exponent with which the stress depends on the strain rate is usually not so different between the Transition and the Critical regime, 0.25 and 0.36 respectively[1]. These two factors can conspire to make the Transition regime simply look like the crossover from the Yield to the Critical regime, especially when noise is an issue, as it often is in experiments. Therefore, the lack of an obvious Transition regime is not immediately worrying.

Thirdly, and still more problematic is the analysis that Katgert performs in his later paper [34] to determine the dependence of the stress on the density. He finds two main results: the exponent β does not depend on the density but a prefactor that he calls k does via $k \sim \Delta\phi^{-1}$. The fact that β does not depend on $\Delta\phi$ is fully consistent with the results from our model, see Eq. 7.17, but the result for k is problematic. Using the definitions of Katgert *et al.* $k \sim \Delta\phi^{-1}$ can be translated to $\sigma \sim \Delta\phi$ in our language, however our model predicts that σ is independent of $\Delta\phi$ in the Critical regime. According to Katgert, this dependence of the viscous force on the density is a consequence of the fact that the viscous force between two bubbles also depends on their overlap: bubble pairs with a bigger overlap have a bigger contact surface and therefore experience more drag from each other. Our model does not account for this property of the forces between bubbles and therefore it is not strange that we do not predict its consequences, but that is a weakness in the model nonetheless.

The most reasonable approach might be that our model takes into account all sources of strain rate or velocity dependence in foams and is therefore able to predict the dependence of the stress on the strain rate correctly. However, the model does not correctly take into account all sources of density or overlap dependence, leading to incorrect predictions concerning the dependence of the the stress on the density. If this is indeed the correct way to look at the results above, then our model should correctly predict the density dependence in a system where there are no density effects that are unaccounted for in our model, like colloids.

7.5.2 Nordstrom Colloid Data

The second experimental system that we look at is the colloidal system of Nordstrom *et al.* [39]. In this system, N-isopropylacrylamide, or NIPA, colloidal particles of about a μm in size are forced through a tube of size L by a pressure difference, ΔP between the ends of the tube, see figure 7.2 **a**. The particles are suspended in water and, since they swell by absorbing water, they are nearly index and density matched with the water. Due to the change in

[1]These values are found by substituting the experimental value of $\alpha_v = 2/3$ into the relation for the stress in the Transition regime as given in in table 7.1.

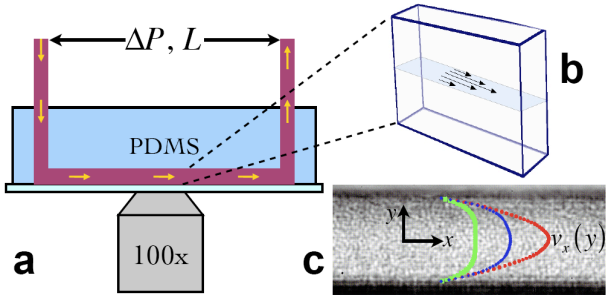

Figure 7.2: Schematic of the microfluidics setup used by Nordstrom *et al.* **a** Side view of the setup. **b** horizontal slice at half height in the channel, showing an example velocity profile. **c** Real data example, showing three example velocity profiles. Figure from [39]

stress as a function of the coordinate perpendicular to the direction of flow, y, the strain rate will also depend on y. Since the strain rate itself is the spatial derivative of the velocity profile, Nordstrom *et al.* were able to obtain the strain rate at different points in their setup by numerically differentiating their velocity profiles, some examples are shown in figure 7.2 **c**. Stress and strain rates as a function of position in the channel can then be combined into a rheological curve linking stress and strain rate directly. This novel technique allows them to get a full rheology curve for a particular density from only one experiment.

Following Olsson & Teitel [11] and the original predictions of our 3E model, [33], Nordstrom *et al.* plot their rheological data in a collapse plot, shown in figure 7.5.2. As can be seen from the figure they find good collapse when plotting $\sigma/\Delta\phi^{2.1}$ vs. $\dot{\gamma}/\Delta\phi^{4.1}$, finding an exponent of the stress in the Critical regime of $\beta = 0.48$

This rheological curve can be compared to our theoretical predictions if we know the microscopic interactions between NIPA particles. Nordstrom *et al.* claim that their particles have simple linear viscous drag, but that they have hertzian elastic interactions, meaning that $F^{\mathrm{e}}_{ij} \sim \delta^{3/2}_{ij}$, or $\alpha_{\mathrm{e}} = 3/2$. Substituting these values into our model gives an exponent in the Critical regime, β, of

$$\frac{\alpha_{\mathrm{v}}(1+\alpha_{\mathrm{e}})}{2+\alpha_{\mathrm{v}}+\alpha_{\mathrm{e}}} = \frac{1+3/2}{2+1+3/2} = 5/9 = 0.55. \tag{7.32}$$

The question of the correct exponents of $\Delta\phi$ to obtain collapse, Δ and Γ in the language of Nordstrom *et al.* , is a little bit more complicated, as there are three options, collapsing any two of the three regimes, Critical, Transition and Yield. We obviously have collapse in the Critical regime and the authors consider the Yield stress collapsed, so we should look at our predictions for collapsing the Critical and Yield regimes. With the exponents for these colloids

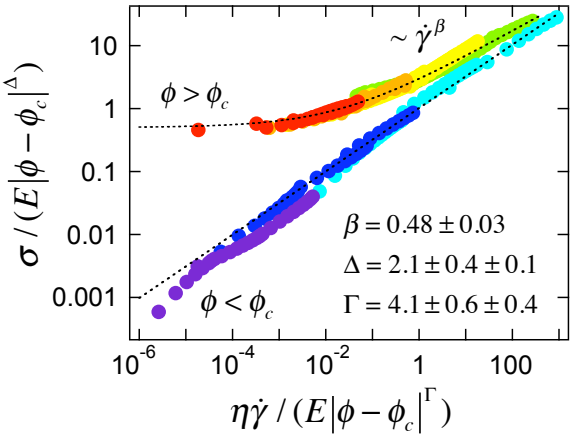

Figure 7.3: Stress and strain rate from the colloidal experiments of Nordstrom *et al.* E denotes the bulk modulus, η the viscosity of the water. Figure from [39]

substituted, we predict that we get collapse for

$$\Delta = 2 \tag{7.33}$$
$$\Gamma = 3.6 \tag{7.34}$$

These values for Δ and Γ agree quite well with the experimental results of Nordstrom *et al.* , $\Delta = 2.1 \pm 0.4$ and $\Gamma = 4.1 \pm 0.6$. Our predicted value of β, 0.55, is outside the experimental range of 0.48 ± 0.03 though. This is strange because, $\beta = \Delta/\Gamma$. However, Nordstrom *et al.* don't get β from the collapse plot, they get it by fitting datasets at a fixed density to the following Herschell-Bulkely expression:

$$\sigma_{xy} \sim \sigma_y + \dot{\gamma}^{\beta}, \tag{7.35}$$

in which σ_y is a yield stress. This expression does not properly account for the Transition regime and trying to fit data that is partially in the Transition in stead of in the Critical regime will result in a value for β that is closer to the Transition exponent of 0.42. Since it is extremely likely that at least the red dataset in figure 7.5.2 is in the Transition regime, it is not surprising that Nordstrom *et al.* find an exponent of 0.48 in between the Transition exponent of 0.42 and the Critical exponent of 0.55.

7.5.3 Conclusion

We have extended our 3E model to nonlinear microscopic interactions. We have compared the predictions of that model with the results of two experi-

ments: the foams of Katgert, which have nonlinear viscous interactions and the colloids of Nordstrom, which have nonlinear elastic interactions. In both cases the model performed well. However, in both cases there were some issues, specifically the presence or absence of a Transition regime. In order to be able to study this in more detail and for a wider range of microscopic exponents, we would like to perform computer simulations again. These are discussed in the next chapter.